GNSS/INS Tightly Coupling System Integrity Monitoring by Robust Estimation

Article *in* Journal of Aeronautics, Astronautics and Aviation, Series A · March 2018

DOI: 10.6125/JoAAA.201803_50(1).06

3 authors:

Shizhuang Wang
Shanghai Jiao Tong University
19 PUBLICATIONS **44** CITATIONS
SEE PROFILE

Xingqun Zhan
Shanghai Jiao Tong University
214 PUBLICATIONS **752** CITATIONS
SEE PROFILE

Weichuan Pan
Qianxun SI
6 PUBLICATIONS **17** CITATIONS
SEE PROFILE

Journal of Aeronautics, Astronautics and Aviation, Vol.50, No.1, pp.061 - 080(2018)
*DOI: 10.6125/*JoAAA.201803_50(1).06

GNSS/INS TIGHTLY COUPLING SYSTEM INTEGRITY MONITORING BY ROBUST ESTIMATION *

Shizhuang Wang, Xingqun Zhan ** and Weichuan Pan

School of Aeronautics and Astronautics, Shanghai Jiao Tong University
No.800, Dongchuan Road, 200240, Shanghai, China

ABSTRACT

Integrity monitoring of the GNSS/INS integrated system is of great importance for safety critical applications. An improved integrity monitoring method for GNSS/INS integrated system which is based on robust estimation is developed in this paper for the purpose of enhancing the ability of fault detection and exclusion. Complete algorithm of fault detection and exclusion based on multi hypotheses innovation separation is built in this paper. The robust estimation and the fault detection and exclusion algorithm are combined to improve the performance of both algorithms. The traditional methods are mostly troubled by the micro and slow growing faults because of the innovations' distortion caused by error tracking of the filter, which brings difficulties to fault detection and exclusion algorithm. Robust estimation is an effective way to reduce the effect of error tracking under micro and slow growing faults by reducing the effect of the faulty measurements and hence to provide more accurate innovations. By using robust estimation in GNSS/INS integrated system, the distortion of the innovations is obviously reduced and the ability of fault detection and exclusion is enhanced. The theoretical analysis and computer simulations prove the performance improvements based on the proposed method.

Keywords: Robust estimation, integrity monitoring, tight coupling, fault detection and exclusion, slow growing faults

I. INTRODUCTION

Integrity of the navigation system has drawn high attention in both civil and military applications. Among the performance specifications of navigation system, including accuracy, continuity, availability and integrity, integrity is most related to safety [1]. Academics and industry are committed to improving the integrity of the navigation system. Aircraft-based Autonomous Integrity Monitoring (AAIM) techniques have been shown to enhance the integrity of the system. Fault detection and exclusion is an important function inside AAIM.

Compared to GNSS-standalone system, a GNSS/INS tightly coupled system can provide better performance, including higher precision and higher integrity [2]. Hence, GNSS/INS integrated system is of significance for safety critical operations, such as APV-II and CAT-I. Integrity monitoring of the integrated system is of great importance because of the possible errors in both GNSS and INS systems, which are troubling for the performance of the integrated system. [3]

There are many studies focusing on the integrity monitoring methods for the integrated system, especially the fault detection and exclusion algorithm. The autonomous integrity monitoring methods can be divided into two parts: measurement-based methods, such as chi-square test, w-test, Autonomous Integrity Monitored Extrapolation (AIME) [4] and Extended RAIM (eRAIM) [5] algorithms; solution-based methods, such as Multiple Solution Separation (MSS) method [6]. The integrity monitoring methods can also be divided into "snap-spot" algorithm where only the current information is used and

* Manuscript received, January 14, 2018, final revision, February 27, 2018
** To whom correspondence should be addressed, E-mail: xqzhan@sjtu.edu.cn

"sequential" algorithm where both the current information and the past information are used. AIME is a typical "sequential" algorithm while MSS is a "snap-spot" algorithm. "Sequential" algorithms have better performance in detecting tiny faults and slow growing faults than "snap-spot" algorithms. [7]

There are two major difficulties existing in integrity monitoring of GNSS/INS integrated system: one is the time delay in detecting the tiny faults and the slow growing faults, and the other is the identification and exclusion of multi failures. If these difficulties can't be solved properly, the performance of the navigation system will be in danger.

Hence, they have attracted much attention of the scholars recently. This paper focuses on these two difficulties, too.

Zhong et al. found that the innovations' distortion caused by the effect of "error tracking" is one of the major causes of the two difficulties. [8] Robust estimation is an effective way to ensure the accuracy and reliability when faults occur to the system and it is useful in integrity monitoring. Yang proposed an idea of using M-estimator in RAIM algorithm to enhance the ability of fault detection and exclusion for GNSS standalone system. [9] Li applied robust estimation and extrapolation-accumulation method in RAIM algorithm to shorten the detection time of micro and slow growing biases of GNSS system. [10]

This paper proposes a new integrity monitoring method for GNSS/INS integrated system based on robust estimation for the purpose of enhancing the ability of fault detection and exclusion, i.e. to shorten the time delay in fault detection and improve the accuracy rate of fault exclusion. The method in this paper combines the robust estimation algorithm with fault detection and exclusion algorithm to improve the performance of both algorithms. The algorithm in this paper also uses the multi hypotheses innovation separation method to enhance the ability of fault detection and exclusion and this idea is enlightened by Multi Hypotheses Solution Separation (MHSS) ARAIM algorithm, although ARAIM is a solution-based method.[11] This paper provides an approach to deal with the two difficulties shown above.

This paper is organized as follows: Section II briefs the basic principle of GNSS/INS tightly coupled system and robust estimation. Section III builds the integrity monitoring algorithm, especially the fault detection and exclusion algorithm, for the integrated system and analyzes the effect of robust estimation on reducing the effect of "error tracking" and enhancing the ability of fault detection and exclusion. Section IV gives some simulations to verify the statements in the previous sections. Section V draws the conclusions.

II. GNSS/INS TIGHTLY COUPLED ALGORITHM BASED ON ROBUST ESTIMATION

Integrating GNSS with INS is an effective way to provide a continuous, high-bandwidth, complete navigation solution with high accuracy and integrity. Tightly coupled architecture is widely used in the navigation of vehicles. Kalman filter method is currently one of the most popular approach to state estimation. However, real data sets frequently contain outliers, including gross errors or exceptional measurements. In this situation, the Kalman filter becomes unreliable. Robust estimation aims to obtain the reliable state estimates even with the situation of some bad measurements. Appling robust estimation to GNSS/INS integration algorithm is of many benefits, which will be shown in Section III. The closed-loop GNSS/INS tightly coupled algorithm and the robust estimation theory are given in this section.

2.1 GNSS/INS tightly coupled algorithm

A tightly coupled (TC) system uses the GNSS pseudo-range and pseudo-range-rate measurements and IMU measurements as the inputs of the integrated algorithm. In the closed-loop configuration, the estimated position, velocity and attitude errors are fed back to INS processor on each filter iteration to correct the INS solution itself. There is no independent uncorrected INS solution because the Kalman filter's position, velocity, and attitude estimates are set to zero after closed-loop correction. [2] Figure 1 shows the typical architecture of the closed-loop GNSS/INS tightly coupled system.

Then the detailed introduction of this algorithm is given below. The 17-dimension state vector of the error state EKF is composed of the INS estimation errors, the GNSS biases, and the inertial sensor biases.

$$x = [\delta a; \delta v; \delta p; b^a; b^g; b^{clk}; \dot{b}^{clk}],$$

where:

- $\delta a, \delta v$ and δp are the INS estimation errors of attitude, velocity, and position separately, and they are 3x1 vector representing for three directions respectively.
- b^a and b^g are the 3-dimenison accelerator biases and 3-dimension gyro biases of the inertial sensor respectively.
- b^{clk} and $\dot{b}^{clk}$ are the GNSS biases, including clock bias and drift.

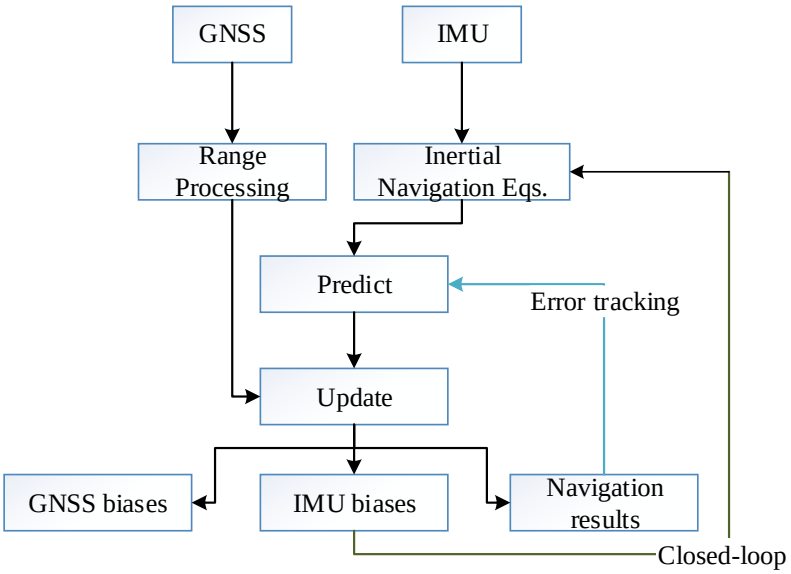

Figure 1 Closed-loop GNSS/INS TC system architecture

In GNSS/INS hybridization model, Kalman filter is used to obtain the state estimates. And the discrete-time state equation has the form as follows:

$$x_{k+1} = \Phi_{k+1|k} x_k + \omega \tag{1}$$

where $\Phi_{k+1|k}$ is defined as the *transition matrix*, which denotes the discrete-time and linearized state transition model built from the dynamic model of the system, i.e., INS error analysis equations; ω is defined as the *process noise vector*, whose covariance matrix is defined as the *system noise covariance matrix*, Q.

The other model of the filter is the system measurement observation, as shown below:

$$z_{k+1} = H_{k+1} x_{k+1} + v \tag{2}$$

where z denotes the *observation vector*, and H denotes the *observation model*, and v denotes the *observation noise vector*, whose covariance matrix is defined as the *measurement noise covariance matrix*, R.

Then we recall the Kalman filter equations to introduce the integration algorithm.

Predict:

$$\hat{x}_{k+1|k} = \Phi_{k+1|k} \hat{x}_k + \omega_k \tag{3}$$

$$P_{k+1|k} = \Phi_{k+1|k} P_k \Phi_{k+1|k}^T + Q_k \tag{4}$$

where P denotes the *error covariance matrix*, which is the covariance matrix of x.

Update:

$$r_{k+1} = z_{k+1} - H_{k+1} \hat{x}_{k+1|k} \tag{5}$$

$$K_{k+1} = P_{k+1|k} H_{k+1}^T (H_{k+1} P_{k+1|k} H_{k+1}^T + R_{k+1})^{-1} \tag{6}$$

$$\hat{x}_{k+1} = \hat{x}_{k+1|k} + K_{k+1} r_{k+1} \tag{7}$$

$$P_{k+1} = (I - K_{k+1} H_{k+1}) P_{k+1|k} \tag{8}$$

where r denotes the *innovations* of the filter, and r plays an important role in fault detection and identification, which will be shown in Section III; K denotes the *Kalman gain matrix*. The state estimates depend on the propagated state estimates $\hat{x}_{k+1|k}$ and the innovations. Consequently, when a fault occurs in GNSS measurements, the state estimates will be affected at once. Besides the basic equations of Kalman filter shown above, the *covariance matrix of the innovations*, S_{k+1} is also important, which is expressed as [12]:

$$S_{k+1} = H_{k+1} P_{k+1|k} H_{k+1}^T + R_{k+1} \tag{9}$$

Note that, the detailed derivation of the algorithm and the expression for the matrices above can be found in many textbooks, including [2].

2.2 Robust estimation theory

The core idea of robust estimation is to decrease the effect of the outliers on the state estimates, and the function of robust estimation can be regarded as "*anti-outliers*" consequently. The equivalent weight function is the very heart of the robust estimation. There are many kinds of equivalent weight function raised in the past years, e.g., Huber function, IGG function and IGG-III function. According to [13], a robust estimator with IGG-III equivalent weight method may be the optimal project among Huber method, IGG method and IGG-III method. Hence IGG-III equivalent weight function is chosen as the selecting weight iteration method of robust estimation in this paper.

In this part, two kinds of robust estimator based on IGG-III equivalent weight method are proposed: one is the "snap-spot" robust estimator to deal with the step errors, and the other is the "sequential" robust estimator to deal with the slow growing errors (SGEs) and the tiny faults. Besides, In GNSS/INS tightly coupled system, Kalman

filter is use as the state estimation method. Hence the robust estimator for GNSS/INS tightly coupled system should be based on KF, too. The two robust KF estimators are shown as follows:

"Snap-spot" robust estimator

According to idea of robust estimation, the equivalent weight of one measurement in estimating the state should be reduced if a fault occurs to it. This function can be realized simply by adjusting the Kalman gain matrix *K*. The robust Kalman gain K_R is expressed as:

$$K_R = K \cdot W \tag{10}$$

where *W* is the equivalent weight matrix, and *W* is a diagonal matrix whose diagonal elements are the equivalent weight of each measurements, a_i :

$$\mathrm{W} = \begin{vmatrix} \ldots & 0 & 0 \\ 0 & a_i & 0 \\ 0 & 0 & \ldots \end{vmatrix}, \ i = 1,2,3,\ldots,N \tag{11}$$

where *N* is the number of the measurements.

The value of a_i is determined by IGG-III equivalent weight function, which is shown as below [14]:

$$a_i = \begin{cases} 1 \ , \ |\omega_i| \le k_0 \\ \frac{k_0}{|\omega_i|}\left\{\frac{k_1-|\omega_i|}{k_1-k_0}\right\}^2 , \ k_0 \le \ |\omega_i| \le k_1 \\ 0 \ , \ |\omega_i| \ge \ k_1 \end{cases} \tag{12}$$

where ω_i is the normalized innovation of the i-th measurement. Because the mean value of the innovation is zero, ω_i can be expressed as:

$$\omega_i = \frac{r^i}{\sigma_{r^i}} \tag{13}$$

where r^i is the innovation of the i-th measurement, and σ_{r^i} is its normalized variance, which is determined by the covariance matrix of the innovation S. If there is no fault in the system,

$$\omega_i \sim N(0,1) \tag{14}$$

Traditionally, robust parameters k_0 and k_1 take the empirical values, $k_0 = 2.5\sim3.5$ and $k_1 = 3.5\sim4.5$. [10] Notice that, the normalized innovations are not only the inputs of robust estimation algorithm but also the inputs of fault detection and exclusion algorithm. Hence, the values of k_0 and k_1 are determined by taking the thresholds in fault detection and exclusion algorithm into consideration. The detailed introduction can be found in Section III.

The basic principle of "snap-spot" robust estimator is stated as below:

(1) The absolute value of the innovation of one measurement will increase to a big value at once if a step error occurs to it;

(2) If the normalized innovation becomes significantly big, i.e., larger than k_0 or k_1, the equivalent weight of this measurement in estimating the state will be reduced or even set to zero.

According to the statements above, "snap-spot" robust is effective for relative big step errors while not effective or not efficient for tiny faults or SGEs. To overcome the drawbacks of "snap-spot" robust estimator, "sequential" robust estimator is raised as follows.

"Sequential" robust estimator

"Snap-spot" method means that only the current measurements are considered while "sequential" method means the current measurements and the measurements of past few epochs, i.e., the measurements in "sliding window", are all considered in the calculation. Hence "sequential" robust estimator can also be called "accumulated" robust estimator and it is designed to be more sensitive to tiny faults and slow growing faults.

The difference of "sequential" method and "snap-spot" method focuses on the calculation of the normalized innovations. Statistical variables ω_i in different epochs are independent with each other and all follow the standard normal distribution. The determination of the normalized innovations in "sequential" method is shown below:

$$\overline{\omega_i} = \frac{1}{L}\sum_{t=k-L+1}^{k} \omega_i \tag{15}$$

$$\omega_i^s = \sqrt{L} \cdot \overline{\omega_i} \tag{16}$$

where k denotes the current epoch and *L* denotes the length of sliding window. ω_i is the normalized innovation shown in Equation (13). $\overline{\omega_i}$ is the *average innovation* while ω_i^s is the *sequential normalized innovation* used to determine the equivalent weight matrix. If there is no fault in the system,

$$\omega_i^s \sim N(0,1) \tag{17}$$

Equation (17) can be derived by using the independence of each measurement.

Then the better performance of "sequential" method than that of "snap-spot" method in dealing with tiny faults and SGEs is proofed as follows.

If the faults in the measurements are "realized" earlier by the robust estimator, the effect of the faults will be smaller. The values of the normalized innovations, ω_i or ω_i^s, determine when the robust estimator can detect the faults and reduce their weights. As a result, the bigger the value of the normalized innovation is, the better the performance of the robust estimator is.

(1) Tiny fault:

Assume that a tiny fault, whose magnitude is *B*, occurs to i-th measurement in the sliding window.

For "snap-spot" method, the normalized innovation ω_i with fault is expressed as:

$$\omega_i = \frac{B+r^i}{\sigma_{r^i}} = b + \omega_i^{nf} \quad (18)$$

Where, r^i is the innovation without fault, σ_{r^i} is the normalized variance of r^i and ω_i^{nf} is the normalized innovation without fault as is shown in Equation (13). Variable b is called "normalized magnitude" of the fault in this paper, which is equal to the value of the actual magnitude B over the normalized variance σ_{r^i}.

For "sequential" method,

$$\omega_i^s = \frac{1}{\sqrt{L}}\sum_{t=k-L+1}^{k}\omega_i = \sqrt{L}\cdot b + \omega_i^{sf} \quad (19)$$

Where, ω_i is expressed as Equation (18) and ω_i^{sf} is the sequential normalized innovation without fault as is shown in Equation (16).

Obviously, variable ω_i and variable ω_i^s both follow eccentric standard normal distribution with the eccentric parameters of b and $\sqrt{L}\cdot b$ separately.

$$\frac{\omega_i^s}{\omega_i} \approx \sqrt{L}, \mathrm{L} > 1 \quad (20)$$

The ability of dealing with tiny fault of "sequential" method is about $\sqrt{L}$ times stronger than that of "snap-spot" method because the value of the normalized innovation in sequential method is about $\sqrt{L}$ times larger than that of the "snap-spot" method in the same tiny-fault situation.

(2) Slow growing errors:

Assume that a ramp error whose actual magnitude increase from A to B and normalized magnitude increases from a to b in the sliding window occurs to i-th measurement, and the change rate of the normalized magnitude keeps constant. The derivation is similar to the case of tiny fault.

For "snap-spot" method,

$$\omega_i = \frac{B+r^i}{\sigma_{r^i}} = b + \omega_i^{nf} \quad (21)$$

For "sequential" method,

$$\omega_i^s = \frac{1}{\sqrt{L}}\sum_{t=k-L+1}^{k}\omega_i = \frac{a+b}{2}\sqrt{L} + \omega_i^{sf} \quad (22)$$

If $a\cdot b \geq 0$ and L is sufficiently big,

$$\frac{\omega_i^s}{\omega_i} > 1 \quad (23)$$

That is to say, "sequential" method has a better performance in dealing with slow growing errors in most cases if L is sufficiently big, such as $L \geq 10$.

This derivation also reveals that the ability of "sequential" method in dealing with tiny faults or SGEs increases with the increase of "effective length", i.e. L, of the sliding window while the computational efficiency of the method decreases. "Effective length" means only the length of the window that contains faulty measurements. And L in the analysis above is "effective length". In other words, the length that doesn't contain faulty measurements at one epoch can be called "wasted length" which has negative effect on the performance. Therefore, the length of the sliding window should be not too large nor too small. The length should be determined according to the concrete situation.

III. RESULTS AND DISCUSSION

Integrity of the navigation system is an important performance index in aviation. Airborne autonomous integrity monitoring is an effective approach to enhance the integrity. Fault detection and exclusion (FDE) is the core function of the integrity monitoring algorithm. With FDE, the navigation system can be fault-tolerant by detecting the faults and removing the error measurements when faults occur to the system. In this section, the integrity monitoring algorithm for the GNSS/INS tightly coupled system based on robust estimation is raised, and the influence of the robust estimation on the ability of FDE is analyzed.

3.1 Fault detection and exclusion(FDE) theory

The function of fault detection is to alarm when faults occur to the navigation system and the function of fault exclusion is to identify the faulty measurements and remove them from the filter. Fault detection and exclusion is realized based on the statistics and probability theory, especially the hypothesis testing theory. The detailed algorithm of FDE is shown as follows:

Establish hypotheses

In this paper, multi hypotheses are established to realize the FDE function. The hypotheses are divided into three classes:

(1) Null hypothesis: there is no fault in the system.
(2) Single-fault hypotheses: there is one fault in the system, and each possible location of fault corresponds to one hypothesis.
(3) Multi-faults hypotheses: there are more than one faults in the system, and each possible failure group corresponds to one hypothesis.

It is necessary to determine the *maximum number of simultaneous faults* N_{max} to avoid monitoring unnecessary failure groups. This idea is enlightened by ARAIM algorithm. [11] N_{max} can be determined using the following algorithm.

$$N_{max} = \max(N1_{max}, N2_{max}) \quad (24)$$

where $N1_{max}$ is obtained from ARAIM algorithm, using the prior probability of each measurement [11]; $N2_{max}$ is determined by the actual measurements, and it is equal to the number of satellites whose measurements' equivalent weight is reduced in the robust estimator.

The number of all the hypotheses, N, is expresses as:

$$N = \sum_{i=0}^{N_{max}} C_n^i \quad (25)$$

where, n is the number of the visible satellites.

Test statistics and thresholds

Building the *test statistics s* and calculating the *detection threshold T* is the core part of FDE algorithm. In this paper, innovations are used to build the test statistics. For different kinds of hypotheses, the test statistics and thresholds are different. The detailed algorithm is give as follows:

(1) Single-fault detection:

For single-fault cases, standardized normal distribution is used to establish the test statistics and the thresholds.

$$s = \omega_i \tag{26}$$

where ω_i is the normalized innovation of i-th measurement.

· If there is no fault in i-th measurement,

$$s \sim N(0,1) \tag{27}$$

· And if there is a fault in i-th measurement,

$$s \sim N(\delta, 1) \tag{28}$$

In this case, the detection threshold can be determined as follows:

$$P_{fa} = \int_T^{\infty} p(x)dx \tag{29}$$

where P_{fa} denotes the false alarm probability, which is determined by the requirements of continuity; $p(x)$ is the probability density function of the standardized normal distribution.

If $s \geq T$, we treat i-th measurement as faulty, with a false alarm rate of P_{fa}.

(2) Multi-fault joint detection:

For multi-faults case, chi-square distribution is used to establish the test statistics and the thresholds.

$$s = \sum_i^N {\omega_i}^2 \tag{30}$$

where N is the number of the faulty measurements in this multi-faults hypothesis.

· If there is no fault in the corresponding measurements of this hypothesis,

$$s \sim \chi^2(N) \tag{31}$$

· If there are one or more faults in these measurements,

$$s \sim \chi^2(\lambda, N) \tag{32}$$

where $\chi^2(\lambda, N)$ denotes non-central chi-square distribution with a freedom of *N* and non-central parameter of λ.

In this case, the detection threshold can be determined as follows:

$$P_{fa} = \int_T^{\infty} p(x)dx \tag{33}$$

Here $p(x)$ denotes the probability density function of the chi-square distribution with a freedom of *N*.

There is a question, is it necessary to build multi-faults hypotheses? Here gives the explanation of this question:

Using single-fault hypothesis only is able to detect and exclude the multi faults one by one, but using multi-faults hypotheses can detect and exclude the multi faults simultaneously and the detecting time is less than that of using single-fault hypotheses. This statement will be proofed in the simulation in Section IV.

"Sequential" FDE algorithm

"Sequential" fault detection and exclusion algorithm aims to detect and exclude the ramp errors and tiny errors faster than the "snap-spot" FDE algorithm. The idea of this algorithm is similar to that of AIME (Autonomous Integrity Monitoring Extrapolation), which is shown in [4]. And the better ability of "sequential" algorithm in detecting and excluding SGEs can be proofed just like the proof in "sequential" robust estimator in Section II.

To obtain the "sequential" test statistics, the normalized innovations ω_i should be replaced with the sequential normalized innovations w_i^s. Definition of ω_i and w_i^s can be found in Section II. The detection thresholds of the "sequential" algorithm are the same as that of "snap-spot" algorithm, because the distribution of ω_i is the same as that of w_i^s.

Determine robust parameter

In Section II, the robust parameters, k_0 and k_1, are said to be determined by taking the thresholds in fault detection and exclusion algorithm into consideration. After giving the FDE algorithm, the determination of the robust parameters is given below:

The value of k_1 takes the threshold *T* calculated in the single-fault hypothesis, and the value of k_0 is determined by:

$$k_0 = \kappa \cdot k_1 \tag{34}$$

where κ is an empirical parameter, which has an obvious influence on the performance of the robust estimator:

$$0 < \kappa < 1 \tag{35}$$

In this paper, take $\kappa = 0.5$. It is a common value of k0 over k1 according to the empirical parameters in [10] and [14].

It is easy to find that, "fault exclusion" is included in IGG-III equivalent weight function, i.e. the weight of a measurement is set to 0 if its normalized innovation is larger than k_1. And that is why the threshold is selected as the value of k_1. Besides, when the statistics in the multi-faults hypothesis is larger than its threshold, the weights of

the corresponding measurements should be set to 0. In this way, the robust estimator is coupled with FDE algorithm, which enhances the ability of fault detection and exclusion and reduces the effect of the failure.

3.2 "Error tracking" of Kalman Filter

In FDE algorithm, the innovations are expected to reflect the actual amplitudes of the occurring faults, which are called "ideal innovations" in this paper. However, the actual innovations are not equal to the "ideal innovations" because of the effect of "error tracking" and closed-loop correction during the prediction and updating process of the filter. "Error tracking" is designed to correct the errors in the measurements to improve the navigation accuracy of the integrated system. But it has a bad influence fault detection and exclusion. "Error tracking" and its influence on the innovations is illustrated in Figure 2.

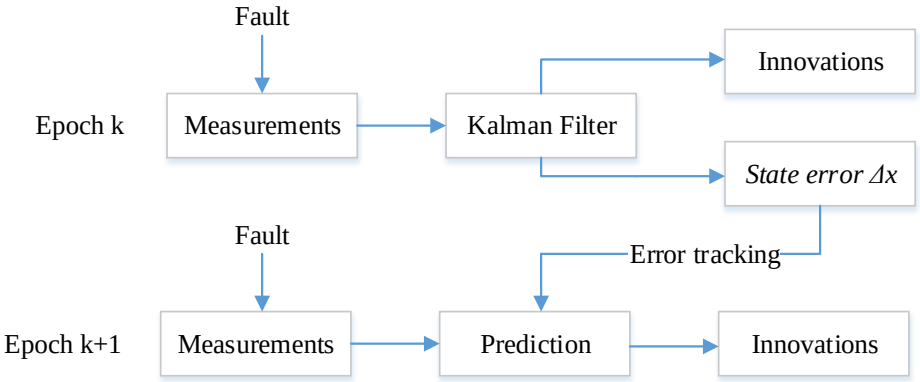

Figure 2 Illustration of "error tracking"

Then the effect of error tracking is analyzed as follows [8, 12]:

Assume that a fault whose amplitude is υ occurs to i-th measurement at epoch k. The fault vector is expressed as:

$$\Gamma = [0 \ \ 0 \ \ 0 \ \ \ldots \upsilon \ \ \ldots 0 \ \ 0]^T \tag{36}$$

where the elements are all zero excepting for the i-th element.

According to Kalman filter theory,

$$\hat{x}_k = \hat{x}_{k|k-1} + K_k r_k \tag{37}$$

$$\hat{x}_k{}^{wf} = \hat{x}_k + K_k \Gamma \tag{38}$$

where $\hat{x}_k{}^{wf}$ denotes actual state estimates at epoch k with a fault in the measurements. The innovations at this epoch can reflect the actual amplitude of fault.

At the next epoch,

$$\hat{x}_{k+1|k} = \Phi_{k+1|k}\hat{x}_k \tag{39}$$

$$\hat{x}_{k+1|k}{}^{wf} = \Phi_{k+1|k}\hat{x}_k{}^{wf} = \hat{x}_{k+1|k} + \Phi_{k+1|k}K_k\Gamma \tag{40}$$

$$r_{k+1} = z_{k+1} - H_{k+1}\hat{x}_{k+1|k} \tag{41}$$

$$r_{k+1}{}^{wf} = z_{k+1} - H_{k+1}\hat{x}_{k+1|k} - H_{k+1}\Phi_{k+1|k}K_k\Gamma \tag{42}$$

therefore,

$$r_{k+1}{}^{wf} = r_{k+1} - H_{k+1}\Phi_{k+1|k}K_k\Gamma \tag{43}$$

where r_{k+1} is the "ideal" innovations that reflect the actual amplitude of the fault, while the actual innovations $r_{k+1}{}^{wf}$ is not equal to the "ideal" innovations.

Define the effect of "error tracking" on the innovations as Δr, which is expressed as:

$$\Delta r = -H_{k+1}\Phi_{k+1|k}K_k\Gamma \tag{44}$$

For a ramp error case or a step error case, the actual innovation corresponding to the faulty measurement is decreased by Δr, and the absolute values of other innovations are increased by $|\Delta r|$. The difference between the actual innovations and the "ideal" innovations caused by "error tracking" decreases the performance of fault detection and exclusion consequently. And the effect of "error tracking" is extremely obvious for slow growing errors because there is time delay to detect the faults and the innovations are affected obviously during the time.

3.3 Robust estimation's effect on FDE ability

In the previous part, the bad effect of "error tracking" on the performance of fault detection and exclusion is analyzed. In this part, a method to reduce the bad influence of "error tracking" is given: using robust estimator in GNSS/INS integrated algorithm. That is to say, robust estimation can enhance the ability of FDE, and the analysis of robust estimation's effect on FDE ability is given as follows:

According the analysis in the previous part, the difference between the actual innovations and the "ideal" innovations, i.e. Δr, is the immediate cause of the decrease of the ability of FDE. Therefore trying to reduce the values of Δr is an effective way to enhance the ability of FDE.

From Equations (10) and (44):

$$\Delta r = -H_{k+1}\Phi_{k+1|k}K_k^R\Gamma = -H_{k+1}\Phi_{k+1|k}(K_k \cdot W_k)\Gamma \tag{45}$$

where equivalent weight matrix W is determined by Equations (11) to (13).

If a fault occurs to i-th measurement, the corresponding weight in matrix W will be small, and the corresponding values in $(K_k \cdot W_k)\Gamma$ will be small. In other words, the values of Δr are reduced by using robust estimation. The mathematic proof is shown below.

Let's combine Equations (10)-(12) and Equations (44)-(45). And we re-label variable Δr without robust estimation as Δr_1 and the other one with robust estimation as Δr_2. For a specific measurement, i-th measurement:

$$\frac{|\Delta r_2(i)|}{|\Delta r_1(i)|} = \alpha_i \tag{46}$$

Where $\Delta r\,(i)$ denotes the i-th term in vector Δr which is corresponding to the i-th measurement. And $|\blacksquare|$ denotes the absolute value of the variable inside the parenthesis. Combine the IGG-III function and the equation above, it is easy to find that robust estimation can reduce the value of $|\Delta r|$ when fault occurs.

The value of $|\Delta r|$ reflects the innovations' distortion caused by error tracking. If the value of $|\Delta r|$ is large, the test statistics of the faulty measurements will be small and the test statistics of the normal measurements will be large according to the analysis in the previous sections. The former effect will lead to difficulties to detect and exclude the faults, and the latter will lead to false detection or false exclusion. These conclusions are verified in the simulation part. Hence we hope that the distortion is as small as possible so that the innovation can reflect the real magnitude of the fault and provide more accurate test statistics. So reducing the value of $|\Delta r|$ leads to the stronger ability of FDE. The effect of $|\Delta r|$ on the ability of FDE is also shown in reference [8] although there is little difference in the methods of FDE between [8] and this paper.

From the analysis above, we can conclude that robust estimation can reduce the effect of "error tracking" and enhance the ability of FDE consequently. The conclusion will be verified in the simulations in Section IV.

IV. SIMLUTION AND DISCUSSION

A MATLAB-Based Simulation Platform was built to study on the performance of the algorithm stated above and verify the statements given in the theoretical analysis parts. The goals of the simulations focus on:

(1) Show the "error tracking" phenomenon and its effect on the innovations;
(2) Give the comparisons of the robust-enhanced algorithm and the traditional algorithm in navigation performance and FDE ability.
(3) In addition, research on the effects of "sequential" robust estimation and "sequential" FDE algorithm.

Note that, robust-enhanced algorithm refers to the algorithm where robust estimation is used in the integration process, while the traditional algorithm refers to the algorithm which uses the classical integration algorithm shown in [2].

4.1 Simulation description

The simulations are done on the MATLAB 2014a software installed on Windows 7 OS. The detailed information about the simulation conditions are illustrated below.

Similar to [2], the GNSS constellation model assumes single constellation, dual frequencies and the circular orbits with satellites equally distributed amongst six orbital planes. There is no simulation of GNSS signal blockage, attenuation, jamming, interference, or reflection.

The error model of GNSS measurements is shown in Table 1.

The parameters below are from [2] with some reasonable changes, e.g. set the ionosphere error SD to 0 because of the dual-frequency correction.

Note that, SD donates standard deviation.

The errors are treated as white noise and the mask angle of the receiver is set to 10 deg.

The information of the parameters of INS in the simulation is shown in Table 2. Note, PSD denotes power spectral density.

The parameters of the Kalman filter are shown in Table 3.

Table 1 GNSS measurement error model

Signal in Space error SD	1m
Zenith troposphere error SD	0.5m
Zenith ionosphere error SD	0 (dual-frequency)
Code tracking error SD	1m
Range rate tracking error SD	0.02m/s
Receiver clock offset (at t=0)	10000m
Receiver clock drift (at t=0)	100m/s

Table 2 Parameters of IMU sensor

Grade	Aviation-grade
Accelerometer noise root PSD	20 $mg/\sqrt{Hz}$
Gyro noise root PSD	0.002 $deg/\sqrt{hr}$
Accelerometer quantization level	5e-5 m/s^2
Gyro quantization level	1e-6 rad/s

Table 3 Parameters of Kalman filter

GNSS update frequency	1 Hz
IMU update frequency	100 Hz
GNSS range error SD	2.5 m
GNSS range rate error SD	0.1 m/s
IMU Gyro noise root PSD	0.004 $deg/\sqrt{hr}$
IMU Accelerometer noise root PSD	40 $mg/\sqrt{Hz}$
Accelerometer bias random walk PSD	3e-9 m^2/s^5
Gyro bias random walk PSD	2e-16 rad^2/s^3

A profile of an aircraft motion at a speed of 200 m/s with two 45^o turns in opposite directions and a 500m climb is used in the simulations. The trajectory file generated by Sprient SimGen can be found in [2]. Figure 3 illustrates the navigation trajectory of the aircraft.

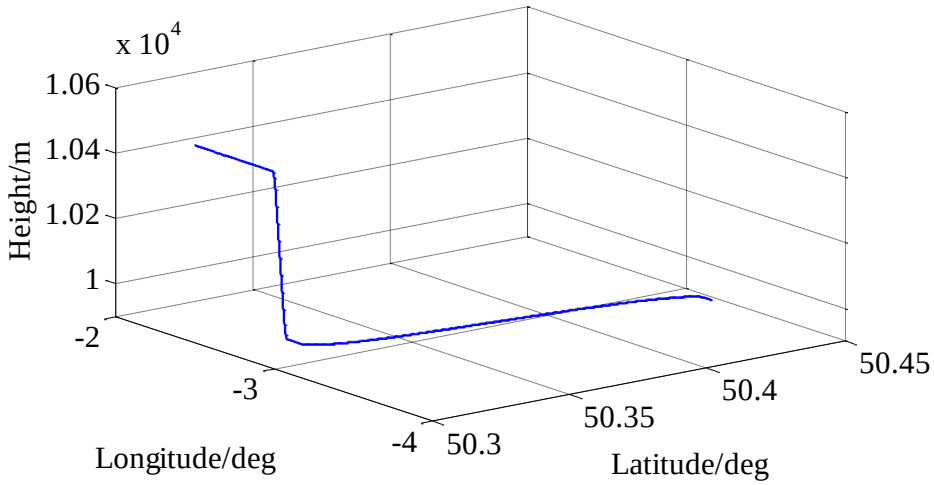

Figure 3 3D plot of the trajectory

4.2 Innovations under step errors and ramp error

To verify the "error tracking" phenomenon and its effect on the innovations, step errors and ramp errors are added to the measurements. The mathematical expressions for the errors are shown below.

· Step error:

$$v(t-k)=\begin{cases} v_f, & if \ \ t \geq k \\ 0 \end{cases} \tag{47}$$

· Ramp error:

$$v(t-k)=\begin{cases} (t-k)\times b_f, & if \ \ t \geq k \\ 0 \end{cases} \tag{48}$$

Where v_f and b_f denote failure magnitude and the slope of ramp error.

Step error

A step failure with a magnitude of 20m is added to the measurement corresponding to No.1 visible satellite from 100s to 250s. The innovations of the measurements without and with robust estimation are shown in Figure 4 and Figure 5, respectively.

Figure 4 shows the effect of "error tracking" on the innovations. Not only are the innovation of the faulty measurement but also the other measurements affected by error tracking. The innovation of the faulty measurement decreases to a value under the true amplitude of the failure and the innovations of the "healthy" measurements increase or decrease to a value with deviations from 0. The sizes of the deviations of different measurements depend on the values of $\boldsymbol{\Delta r}$ in Section 3.2.

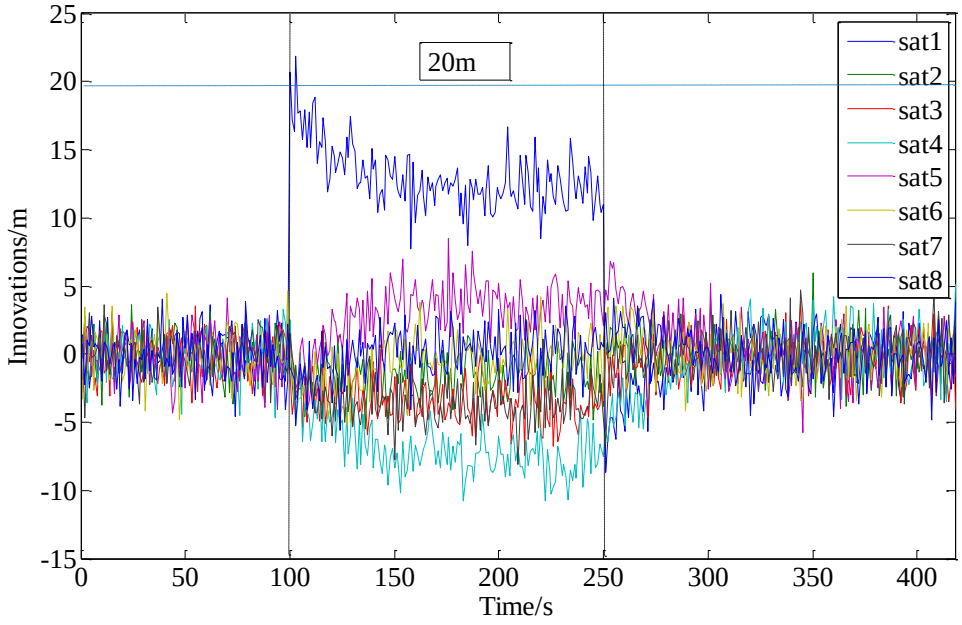

Figure 4 Innovations under step error without robust estimation

Figure 5 displays the effect of robust estimation on reducing the influence of "error tracking". The innovations in Figure 5 tends to reflect the true magnitude of the occurring failure: the innovation of the faulty measurement are close to the fault amplitude with a white noise and the other innovations tend to be unbiased, ignoring the white noise.

The following figures display the multi-failure case.

The same step error is also added to the measurement of No.2 visible satellite at the same time.

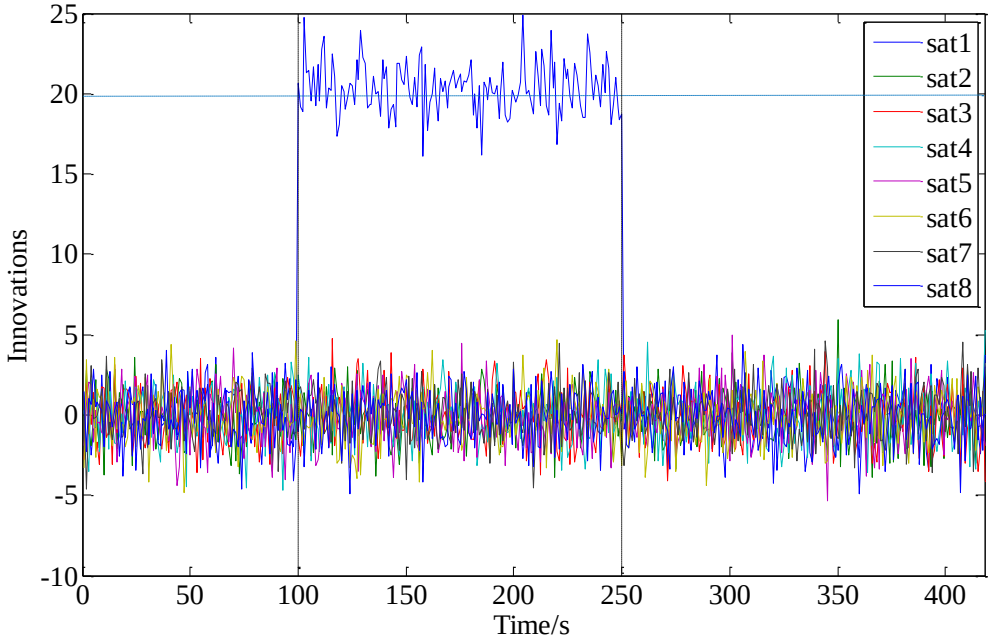

Figure 5 Innovations under step error (robust estimation)

From Figure 6 and Figure 7, we can conclude that robust estimation can also reduce the effect of "error tracking" obviously under multi step errors. And robust estimation can enhance the ability of identifying the faulty measurements and estimating the amplitudes of the failures consequently. This statement will be verified in Section 4.3.

Ramp error

Ramp error is more detrimental for the navigation system than step error because it is hard to be detected. A ramp error with a slope of 0.1m/s is added to the measurement corresponding to No.1 visible satellite from 100s to 250s.

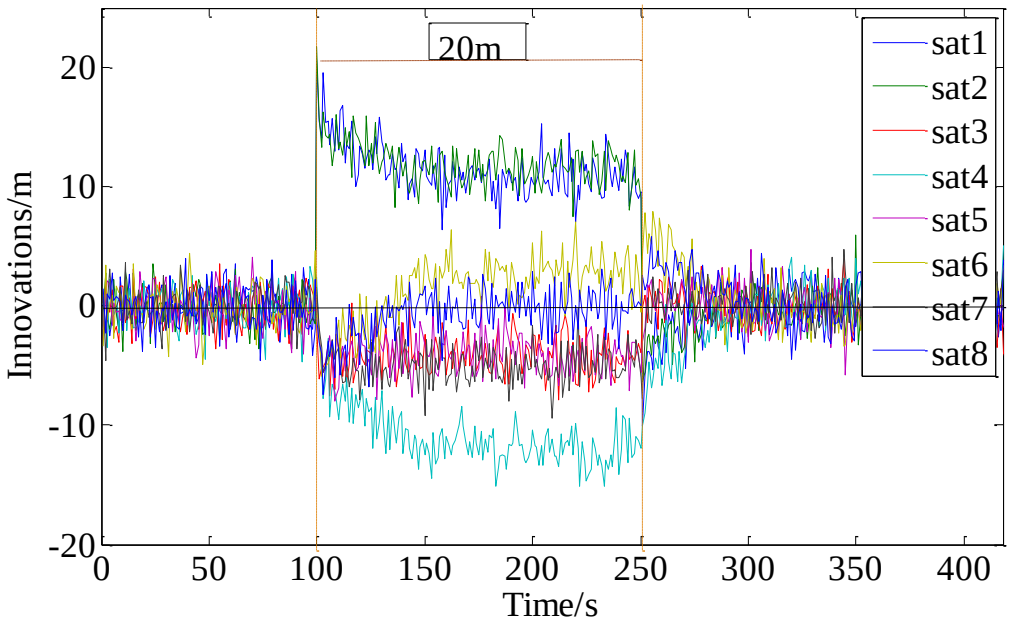

Figure 6 Innovations under multi step errors without robust estimation

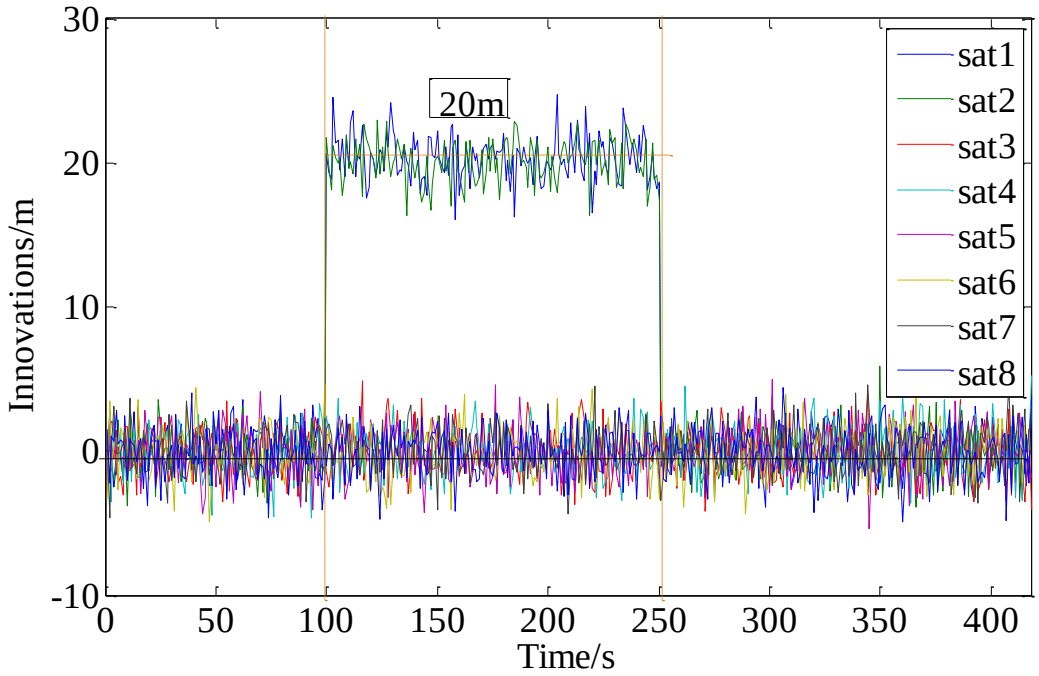

Figure 7 Innovations under multi step errors (robust)

From Figure 8, we can find that the slope of the innovation of the faulty measurement is smaller than that of the true failure. And other innovations are affected by "error tracking" distinctly, too.

From Figure 9 and Figure 10, it is easy to find that the "sequential" robust estimator with a sliding length of 20 epochs has a better performance than that of "snap-spot" robust estimator in reducing the effect of "error tracking" under ramp errors, which corresponds well with the analysis in Section 2.2.

In multi-failure case, the conclusion is similar. To save space, the results of multi ramp faults are not provided here. The multi faults case will be studied in section 4.3.

The simulations in this section verify the effect of "error tracking" and the function of robust estimation in reducing the effect of "error tracking". These conclusions are the immanent cause of the better performance of robust-enhanced algorithm which will be verified in the next section.

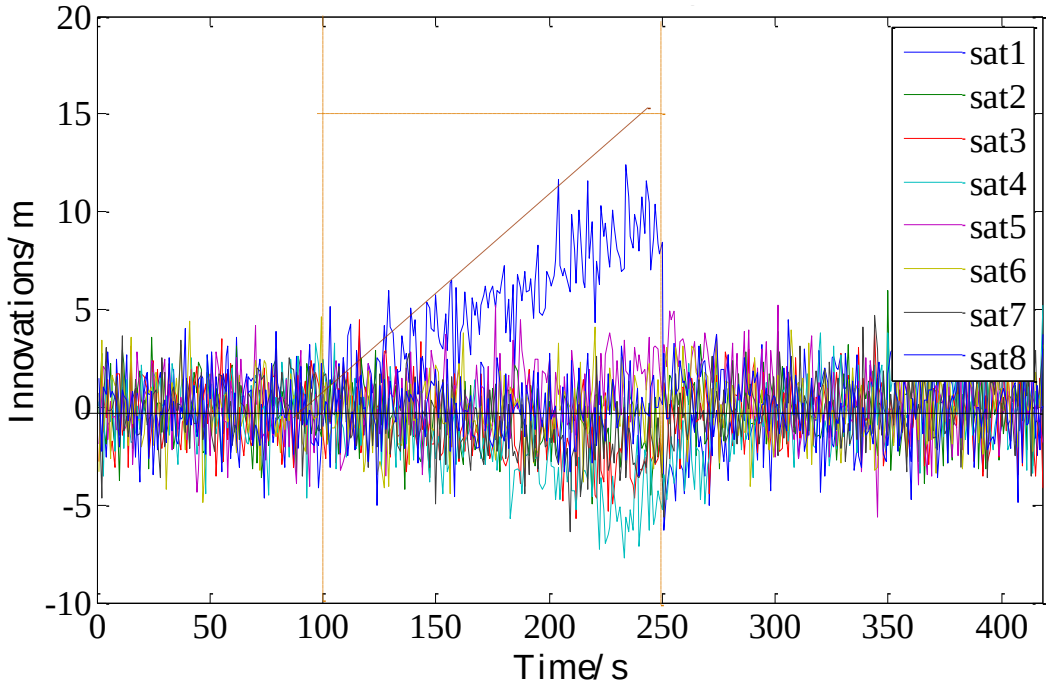

Figure 8 Innovations under ramp error

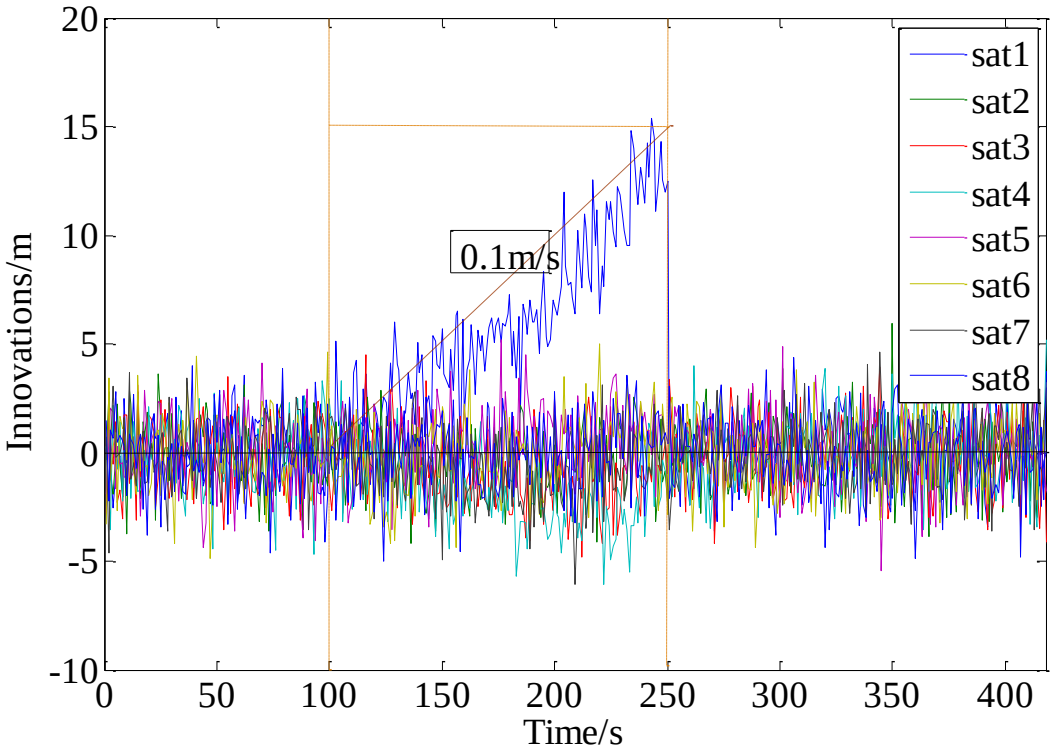

Figure 9 Innovations under ramp error (snap-spot robust)

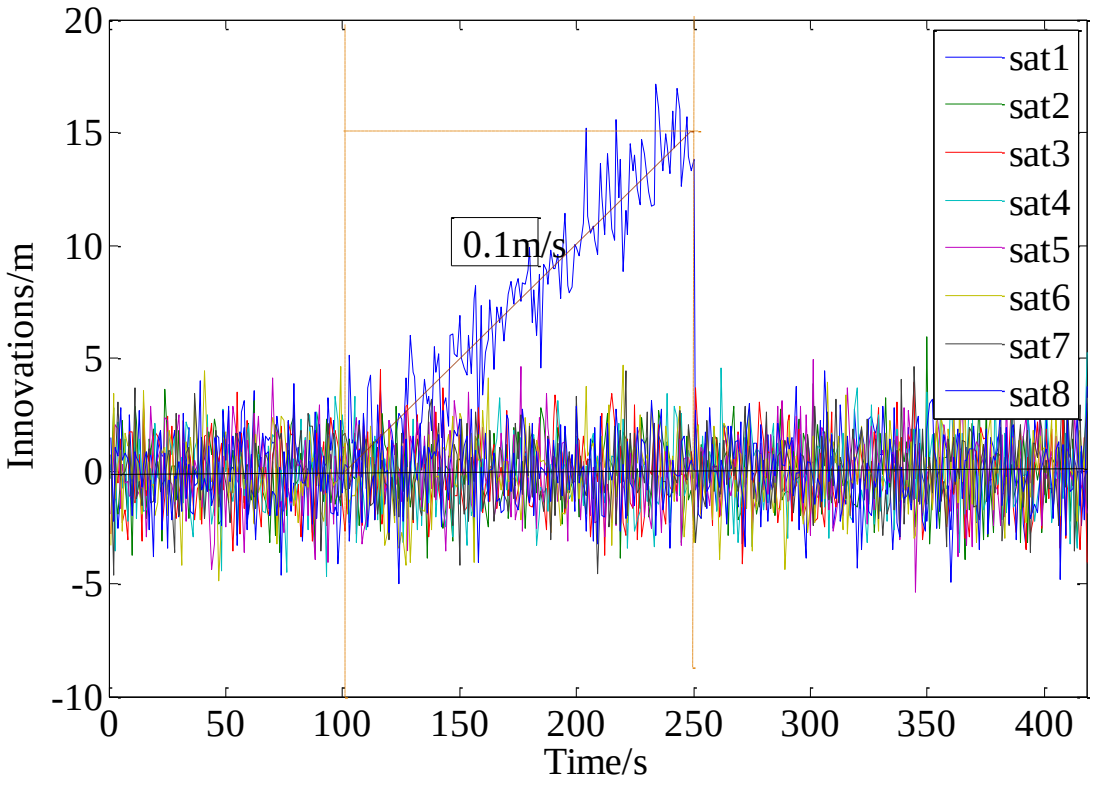

Figure 10 Innovations under ramp error (sequential robust)

4.3 Performance comparisons between robust-enhanced algorithm and traditional algorithm

Robust estimation plays a remarkable role on reducing the effect of "error tracking" and it should show its effect on enhancing the navigation performance and the ability of FDE consequently. In this section, some

simulations are done to prove these analyses. Tiny failures and ramp errors are hard to detect and exclude in real time. Hence the research focuses on these two types of errors and the multi-failure case is analyzed as well.

Tiny failure

A tiny fault with the amplitude of 5m is added to the measurement corresponding to No.3 visible satellite. The integrity monitoring algorithm proposed in Section III is used to detect and identify the fault. The results are shown in the following figures.

Figure 11 shows the test statistics of the measurements where robust estimation is not used in the integrated system. The test threshold is determined using normal distribution and the probability of false alarm. In the simulations, probability of false alarm is set to 1e-8, according to the requirements of continuity. [11] The length of the sliding window to build the statistics is set to 10 in the simulations, according to the analysis of "effective length" in Section 2.2. From Figure 11, it can be concluded that the tiny fault added to the system can't be detected in this case. Figure 12 shows the test statistics of the measurements where sequential robust estimation is used with a sequential length of 10. Robust estimation reduces the effect of "error tracking" obviously, and the innovations are closer to the true amplitudes of the faults. The test statistics of the faulty measurement is the most "distinguished" one among all the test statistics. From Figure 12, it is shown that the tiny fault can be detected and identified correctly with a time delay of about 28s. Figure 13 shows the comparison of the test statistics between the two cases. The effect of "error tracking" and robust estimation on the test statistics is shown clearly in this figure, which strongly proves the previous analyses.

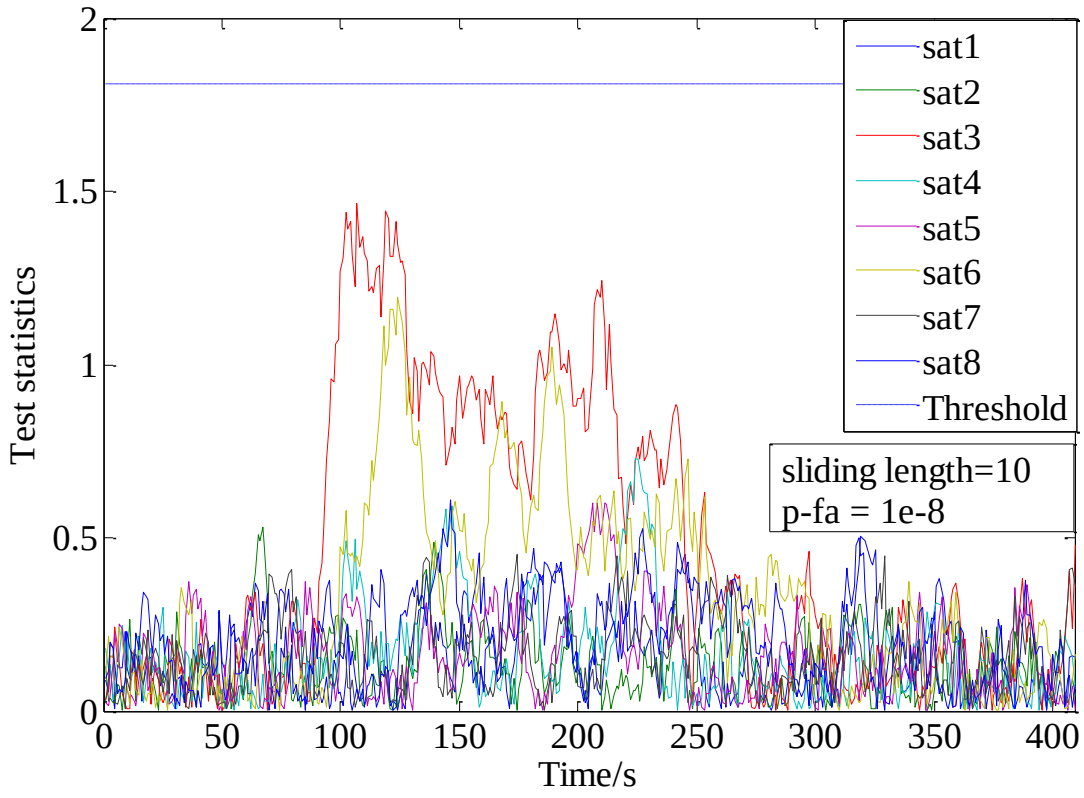

Figure 11 Test statistics under tiny fault (without robust)

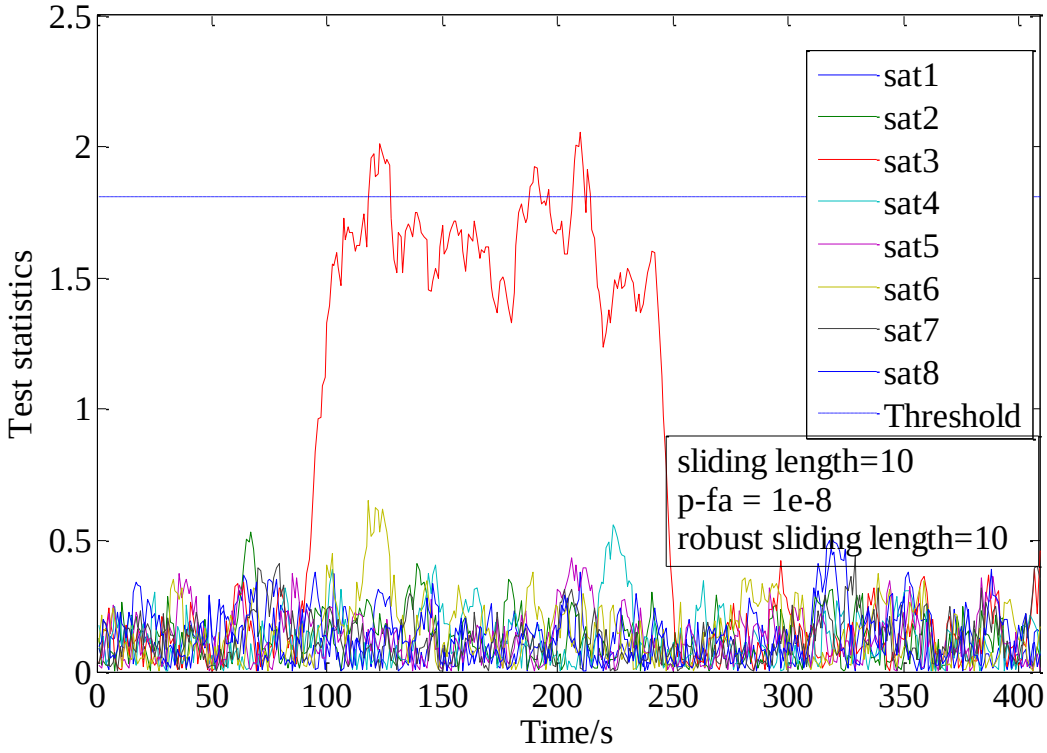

Figure 12 Test statistics under tiny fault (robust)

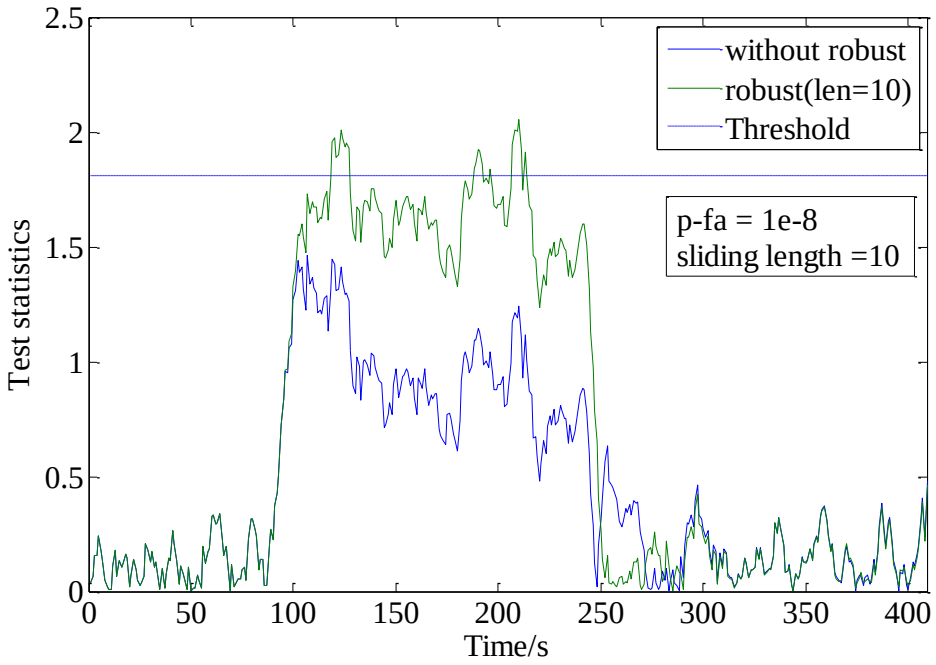

Figure 13 Comparison of test statistics under tiny fault

Ramp failure

A ramp fault with a slope of 0.1m/s is added to the measurement corresponding to the No.3 visible satellite during 100s~250s. The fault can be also called "slow growing error" for its small value of the slope. The simulations try to prove that robust estimation can shorten the time delay to detect the fault.

Figure 14 shows the test statistics under ramp fault without robust estimation in the integrated system. The statistics are somewhat "chaotic" because of the effect of "error tracking". Figure 15 shows the results where robust estimation is used with a sliding length of 20. 20 is a proper value in dealing with the slow growing errors according to the simulations. The test statistics in Figure 15 can reflect the fault clearly, which is good for the fault detection and exclusion process. Figure 16 gives a comparison and

shows that "error tracking" reduces the value of the test statistics of the faulty measurement, and robust estimation reduces the effect of "error tracking". The results show that using robust estimation can shorten the time delay from 91s to 62s, about 30s (1/3 of that of the traditional method), in this case. The effect of robust estimation is very prominent.

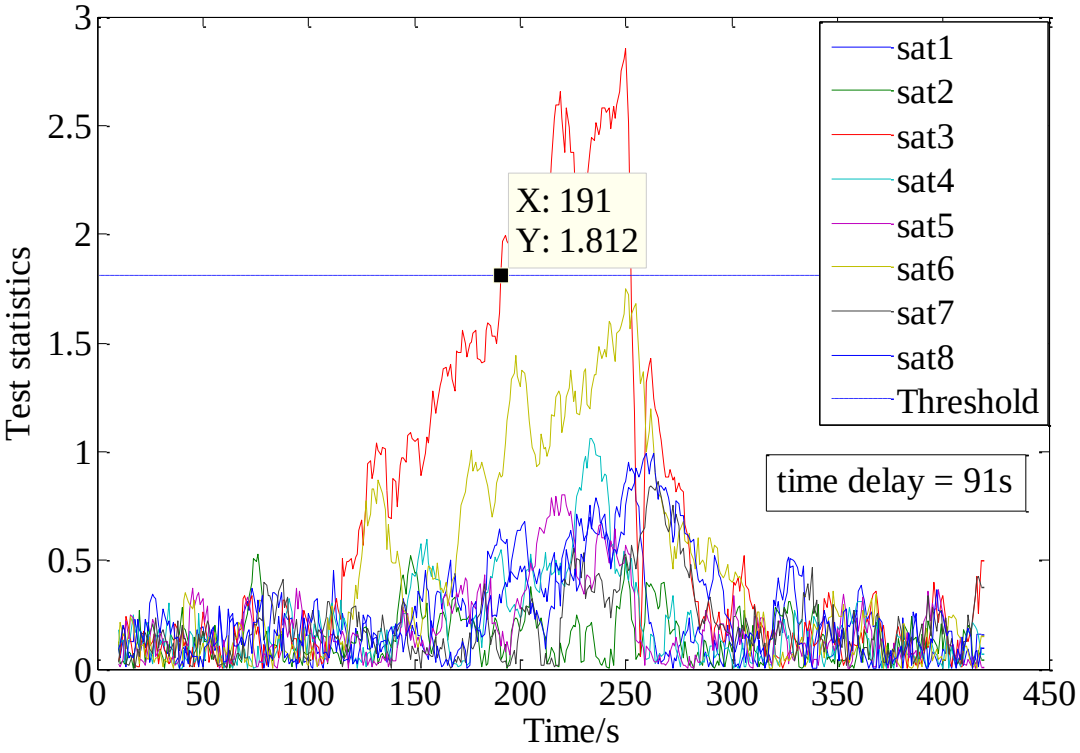

Figure 14 Test statistics under ramp fault (without robust)

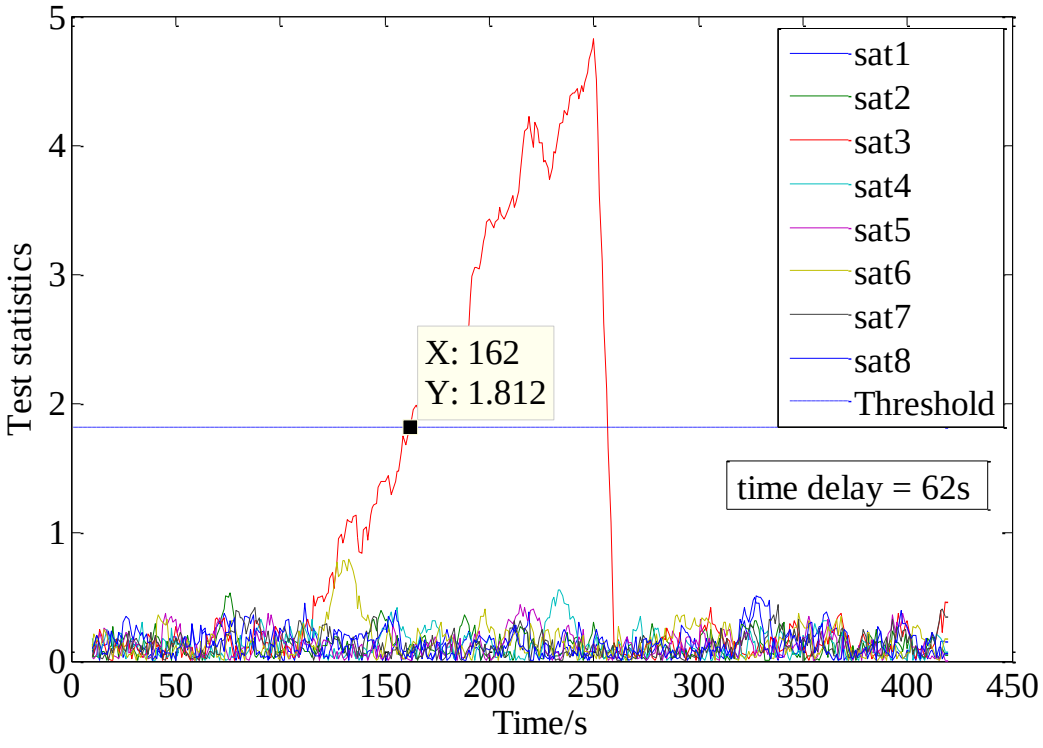

Figure 15 Test statistics under ramp fault (robust)

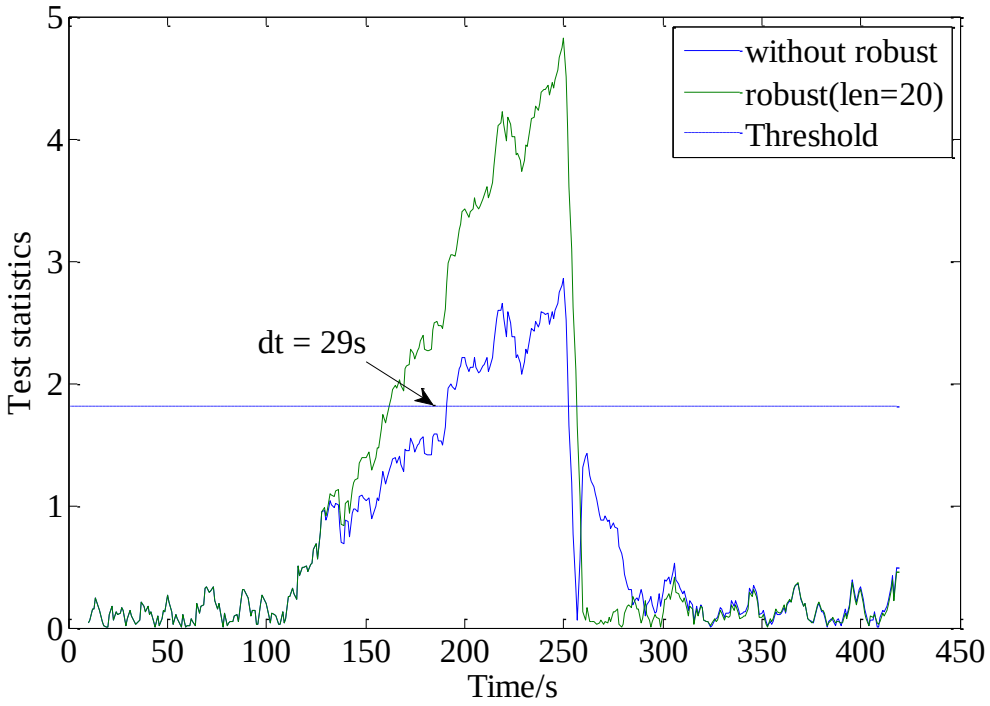

Figure 16 Comparison of test statistics under ramp fault

Multi-failure case

As is stated previously, multi-failure scenarios are a big challenge to the fault detection and exclusion algorithm due to the effect of "error tracking". And we want to prove the effect of robust estimation on enhancing the ability of FDE in multi-failure scenarios using the simulations below.

Ramp faults with the slope of 0.1s are added to the measurements corresponding to No.1 and No.3 visible satellites at the same time from 100s to 250s. Similar to the single ramp fault case, the sliding length of robust estimator is set to 20. Single fault detection and multi-fault joint detection algorithms are both used in the simulations to make a comparison. The algorithms can be found in Section 3.1. The results are shown in Figure 17 and Table 4.

Note that, the test threshold of the multi-fault joint detection is determined using chi-square distribution and the probability of false alarm.

From Table 4 and Figure 17, we can draw the conclusions as follows:

(1) Robust estimation can shorten the time delay of both single fault detection method and multi-fault joint detection method obviously.
(2) Multi-fault joint detection method with robust estimation in the integrated system can detect the faults fast and exclude the faults correctly in multi-fault cases.
(3) For single fault detection method, robust estimation can shorten the time delay of fault detection.

The simulations above prove that the FDE algorithm proposed in this paper with the enhancement of robust estimation can detect the fault(s) fast and exclude it/them correctly in tiny fault(s) and slow growing fault(s) scenarios.

Table 4 The comparison of the time delays.

	Single-1	Single-3	Multi-1&3
Without robust	104s	116s	79s
Robust (len=20)	63s	65s	52s

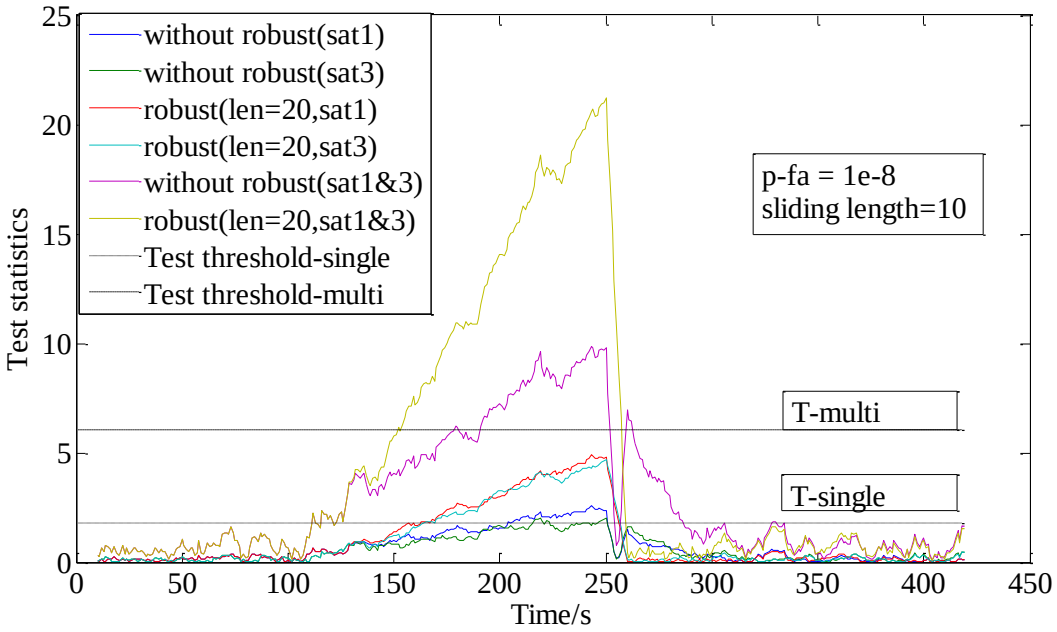

Figure 17 Comparison of test

V. CONCLUSION AND FUTURE WORK

In this paper, a fault detection and exclusion algorithm of the GNSS/INS tightly coupled system based on robust estimation is proposed. The FDE algorithm is based on multi hypotheses innovation separation to detect and exclude both the single fault and multi faults. Robust estimation is used in the integrated system for the purpose of enhancing the ability of FDE in tiny faults and slow growing faults cases. Theoretical analyses and simulations demonstrate that using robust estimation in the GNSS/INS integrated system can reduce the effect of "error tracking" and effectively enhance the ability of FDE in the challenging scenarios: shorten the time delay to detect the tiny faults and slow growing faults, strengthen the ability to detect the tiny faults, and enhance the ability to exclude the faults in both single fault and multi faults cases. The performance improved by the proposed algorithm is useful to enhance the integrity of the navigation system and it is of great significance for civil and military applications.

The future work of this paper focuses on the following points:

(1) Give the sensitivity analysis of the algorithms;
(2) Build the protection level calculation algorithm;
(3) Demonstrate the algorithms using real data.

REFERENCES

[1] Ochieng, W. Y., Sauer, K., Walsh, D., Brodin, G., Griffin, S., and Denney, M., "GPS Integrity and Potential Impact on Aviation Safety," *Journal of Navigation*, Vol. 56, No. 1, 2003, pp. 51-65.

[2] Groves, P. D., *Principles of GNSS, Inertial, and Multi-sensor Integrated Navigation Systems (second edition)*. Artech house, 2013.

[3] Bhatti, U. I. and Ochieng, W. Y., *Improved Integrity Algorithms for Integrated GPS/INS Systems in the Presence of Slowly Growing Errors,* Doctor Thesis, Department of Civil and Environmental Engineering, Imperial College London., 2007.

[4] Diesel, J., and Luu, S., "GPS/IRS AIME- Calculation of Thresholds and Protection Radius Using Chi-square Methods," *Proceedings of the 8th International Technical Meeting of the Satellite Division of The Institute of Navigation (ION GPS 1995)*, 1995, pp. 1959-1964.

[5] Hewitson, S., and Wang, J., "Extended Receiver Autonomous Integrity Monitoring (eRAIM) for GNSS/INS Integration," *Journal of Surveying Engineering*, Vol. 136, No. 1, 2010, pp. 13-22.

[6] Orejas, M., Kana, Z., Dunik, J., Dvorska, J., and Kundak, N., "Multi-Constellation GNSS/INS to Support LPV200 Approaches and Autolanding," *Proceedings of the 25th International Technical Meeting of the Satellite Division of the Institute of Navigation (ION GNSS 2012),* 2012, pp. 790-803.

[7] Liu, H. Y., Feng, C. T., and Wang, H. N., "Method of Inertial Aided Satellite Navigation and Its Integrity Monitoring," *Journal of Astronautics*, Vol. 32, No. 4, 2011, pp.775-780.

[8] Zhong, L., Liu, J., Li, R., and Wang, R., "Approach for Detecting Soft Faults in GPS/INS Integrated Navigation based on LS-SVM and AIME," *Journal of Navigation*, Vol. 70, No. 3, 2017, pp. 561-579.

[9] Yang, Y., and Xu, J., "GNSS Receiver Autonomous Integrity Monitoring (RAIM) Algorithm based on Robust Estimation," *Geodesy and Geodynamics*, Vol. 7, No. 2, 2016, pp. 117-123.

[10] Li, Z., Song, D., Niu, F., and Xu, C., "Receiver Autonomous Integrity Monitoring Algorithm based on Robust Extended Kalman Filter," *Proceedings of IEEE International Conference on Computer and Communications,* 2017, pp. 1809-1813.

[11] Blanch, J., Walter, T., Enge, P., Lee, Y., Pervan, B., Rippl, M., and Spletter, A., "Advanced RAIM User Algorithm Description: Integrity Support Message

Processing, Fault Detection, Exclusion, and Protection Level Calculation," *Proceedings of the 25th International Technical Meeting of the Satellite Division of the Institute of Navigation (ION GNSS 2012),* 2012, pp. 2828-2849.

[12] Giremus, A. and Escher, A. C., "A GLR Algorithm to Detect and Exclude up to Two Simultaneous Range Failures in a GPS/Galileo/IRS Case," *Proceedings of the 20th International Technical Meeting of the Satellite Division of The Institute of Navigation (ION GNSS 2007),* 2007, pp. 2911-2923.

[13] Wang, W., Fan, G., Niu, F., and Xu, C., "Analysis and comparison of robust least squares estimation based on multi-constellation integrated navigation," *Proceedings of IEEE International Conference on Computer and Communications*, 2017, pp. 1752-1756.

[14] Yang, Y. X., "Robust estimation for dependent observation," *Manuscripta geodaetica*, Vol. 19, No. 1, 1994, pp. 10-17.